Cell Reports

Supplemental Information

A Hyperactive Signalosome in Acute Myeloid Leukemia Drives Addiction to a Tumor-Specific Hsp90 Species

Hongliang Zong, Alexander Gozman, Eloisi Caldas-Lopes, Tony Taldone, Eric Sturgill, Sarah Brennan, Stefan O. Ochiana, Erica M. Gomes-DaGama, Siddhartha Sen, Anna Rodina, John Koren III, Michael W. Becker, Charles M. Rudin, Ari Melnick, Ross L. Levine, Gail J. Roboz, Stephen D. Nimer, Gabriela Chiosis, and Monica L. Guzman

Table S1A. List of cell lines. Related to figures 1-4.

Cell Line	Morphology	Type	Karyotype and/or mutation(s)	% Dead (500 nM)
MV4-11	monocytic	AML, M5	FLT3-ITD, MLL-AF4	63.8
MOLM-13	monocytic	AML, M5	FLT3-ITD, MLL-AF9	92.4
THP-1	monocytic	AML, M5	MLL-AF9	16.7
Kasumi-1	myelomonocytic	AML, M2	AML1-ETO, N822K c-kit, TP53 CDK2NA/B	47.2
SKNO-1	myeloblastic	AML, M2	AML1-ETO, N822K c-kit	29.1
M0-91	monoblastic	AML, M0	TEL-TRKC, constitutively active STAT5	97.2
HEL	erythroleukemia	AML	JAK2V617F	19.1
SET-2	megakaryoblastic	essential thrombocythemia	JAK2V617F	75.0
UKE-1	erythroleukemia		JAK2V617F	79.5
KG-1	myeloblastic	AML		31.4
HL-60	promyelocitic	AML	c-myc+, TP53 CDK2NA/B, NRAS	30.5
OCI-AML3	monocytic	AML, M4	NPMc+	19.4
U-937	monocytic	AML, M5	CALM-AF10	26.2
TUR	monocytic	AML, M5	TPA-U937-Resistant	27.0
Kasumi-4	myeloblastic	CML	BCR-ABL	22.8
REH	Lymphoblastic	ALL (non-B, non-T)		6.2

Table S1B. List of COSMIC mutations in cell lines. Related to figures 1-4, S1.

Cell line	Gene	mutation	CDS mutation	Somatic status	Type
TUR	JAK3	p.M511I	c.1533G>A	Previously Reported	Homozygous
TUR	PTPN 11	p.G60R	c.178G>C	Previously Reported	Heterozygous
TUR	TP53	p.?	c.559+1G>A	Confirmed Somatic	Homozygous
TUR	WT1	p.R301*	c.901C>T	Previously Reported	Heterozygous
THP-1	NRAS	p.G12D	c.35G>A	Confirmed Somatic	Heterozygous
Set-2	JAK2	p.V617F	c.1849G>T	Confirmed Somatic	Unknown
Set-2	TP53	p.R248W	c.742C>T	Confirmed Somatic	Unknown
REH	KMT2 D	p.R2140*	c.6418C>T	Previously Reported	Heterozygous
REH	LSM1 4A	p.G439S	c.1315G>A	Previously Reported	Heterozygous
REH	MDM 2	p.S304P	c.910T>C	Previously Reported	Heterozygous
REH	MLH1	p.?	c.790+1G>A	Confirmed Somatic	Homozygous
REH	NOT CH1	p.S2523L	c.7568C>T	Previously Reported	Heterozygous
REH	PRD M1	p.A466T	c.1396G>A	Previously Reported	Heterozygous
REH	TBL1 XR1	p.R166Q	c.497G>A	Previously Reported	Heterozygous
REH	TP53	p.R181C	c.541C>T	Confirmed Somatic	Heterozygous
OCI-AML3	NRAS	p.Q61L	c.182A>T	Confirmed Somatic	Homozygous
OCI-AML3	SMO	p.V157M	c.469G>A	Previously Reported	Heterozygous
MV4-11	POT1	p.K39E	c.115A>G	Previously Reported	Heterozygous
KG-1	NOT CH2	p.K1514R	c.4541A>G	Previously Reported	Heterozygous
KG-1	TP53	p.?	c.672+1G>A	Confirmed Somatic	Homozygous
Kasumi-1	CYLD	p.L773L	c.2319G>A	Previously Reported	Heterozygous
Kasumi-1	KIT	p.N822K	c.2466T>A	Previously Reported	Heterozygous
Kasumi-1	TP53	p.R248Q	c.743G>A	Confirmed Somatic	Homozygous
HL-60	CDK N2A	p.R80*	c.238C>T	Confirmed Somatic	Homozygous
HL-60	NRAS	p.Q61L	c.182A>T	Confirmed Somatic	Heterozygous
HEL	JAK2	p.V617F	c.1849G>T	Confirmed Somatic	Homozygous
HEL	TP53	p.M133K	c.398T>A	Confirmed Somatic	Homozygous

Table S2. List of primary samples. Related to figures 2,3, 5, and 6.

ID	Sample information	FLT3-ITD
AML1	monosomy 7;NPM1 wt; de novo	positive
AML2	M4; Normal cytogenetics; Relapsed	positive
AML3	N/A	positive
AML4	De Novo; M2; Normal cytogenetics	positive
AML5	MDS progression to AML	positive
AML6	N/A	negative
AML7	N/A	negative
AML8	N/A	negative
AML9	N/A	negative
AML10	del(9)(q13)[1] ; De novo	positive
AML11	De Novo, Normal cytogenetics	negative
AML12	De Novo, Normal cytogenetics	positive
AML13	MDS progression to AML, Normal cytogenetics	negative
AML14	MDS progression to AML	negative
AML15	Refractory; 47,XY,+8[3]	positive
AML17	Normal cytogentics	positive
AML18	Normal cytogentics; FLT3-ITD mut/NPM1 mut; de novo	negative
AML19	N/A	positive
AML22	N/A	negative
AML23	CMML evolving to AML; 47,XX,+21[5]/47,XX,+11[3]/46,XX[12]	negative
AML24	De Novo, Normal cytogenetics	negative
AML25	De Novo, Normal cytogenetics	positive
AML27	De Novo, 47,XY,+8[17]/46,XY[3]	negative
AML28	De Novo, Normal cytogenetics	positive
AML29	MDS evolved to AML; Normal cytogenetics	negative
AML30	De novo; Normal cytogenetics	negative
AML34	N/A	N/A
AML35	47,XY,+21[9]/46,XY[11]; De novo	positive
AML33	De novo; Normal cytogenetics	negative
AML37	N/A	negative

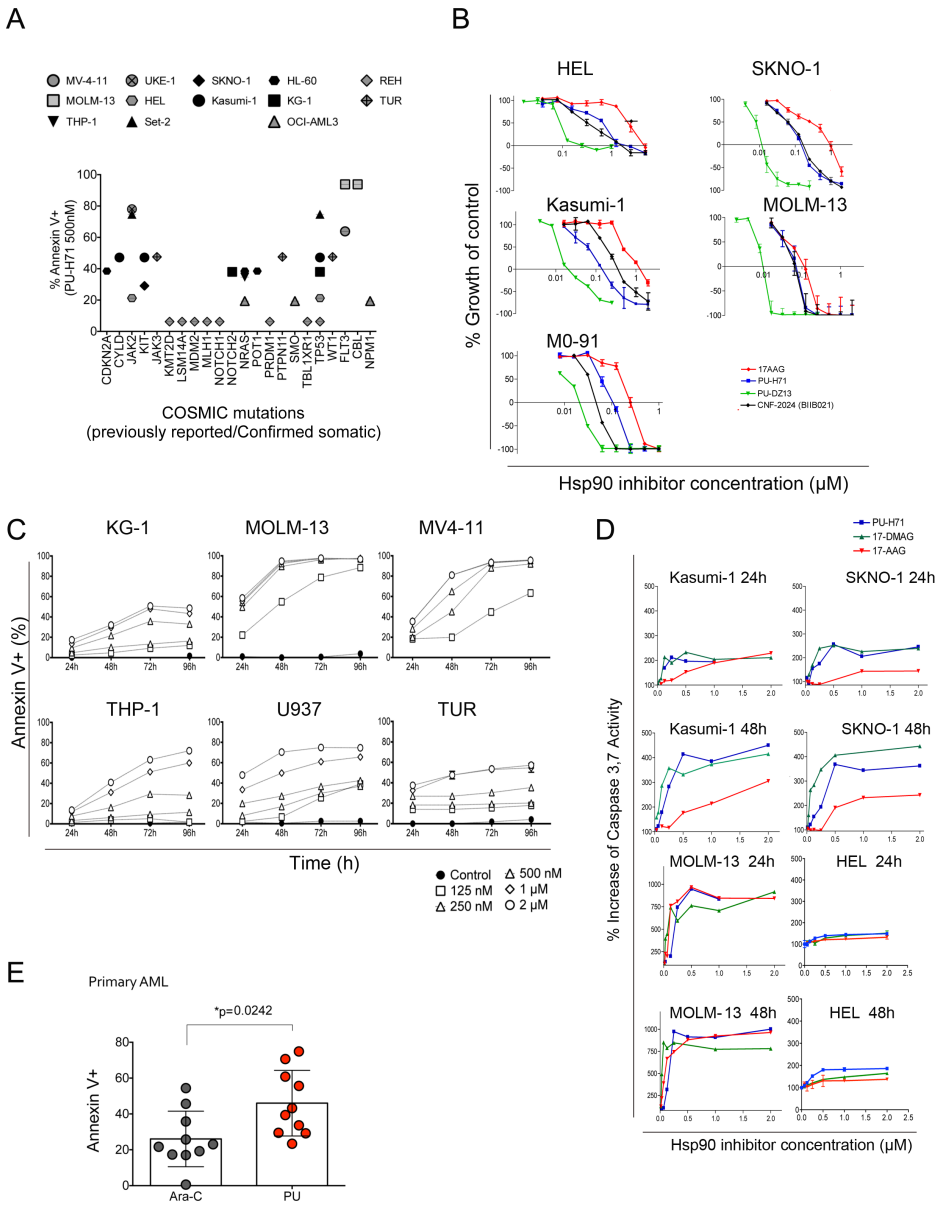

Figure S1. Hsp90 inhibition induces AML cell type-specific death. Related to Figure 1. **(A)** Percent apoptosis after 48h treatment with 500nM PU-H71 relative to control for cell lines tested that have reported/confirmed mutations (COSMIC) See also table S1B. **(B)** HEL, SKNO-1, Kasumi-1, MOLM-13 and M0-91 cells were treated with Hsp90 inhibitors including PU-H71, 17-AAG, PU-DZ13 or CNF-2024 for 72 h. Cell growth was measured by Alamar Blue assay. **(C)** AML cell lines were treated with PU-H71 and evaluated for apoptosis at the indicated time-points. Percent apoptosis was determined by Annexin V staining. **(D)** Percent increase in caspase 3,7 activity assay after 24 or 48 h treatment of Kasumi-1, SKNO-1, MOLM-13 and HEL cells lines with the indicated Hsp90 inhibitors. **(E)** Correlaion between the percent annexin V+ primary AML cells relative to control after 48 h treatment with Ara-C or PU-H71. Each symbol represents a sample.

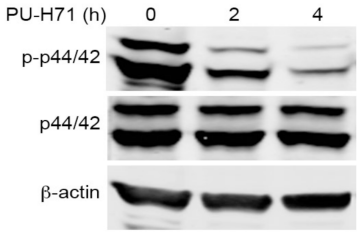

Figure S2. Phosphorylated ERK1/2 is rapidly downregulated by PU-H71. Related to Figure 2. MV4-11 cells were treated with 1 μM PU-H71 for the indicated time points. Immunoblotting was performed using antibodies against phospho-p44/42, total p44/42 and β-actin.

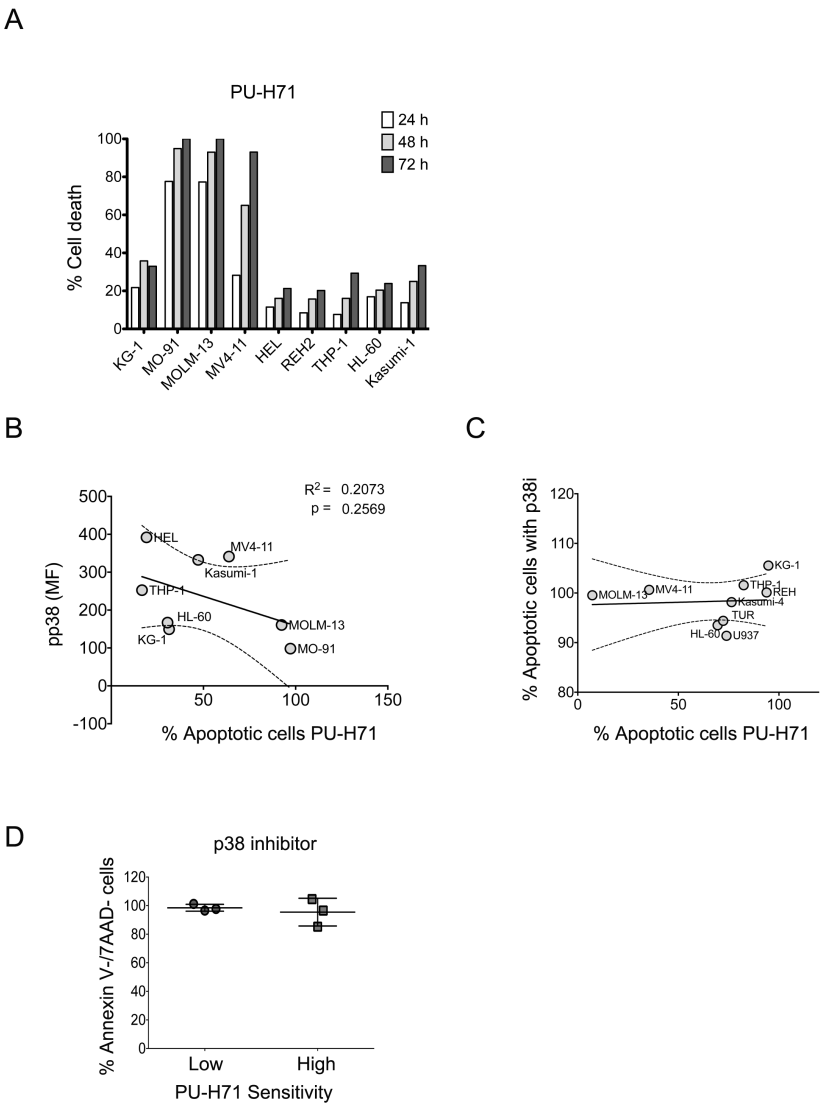

Figure S3. Apoptosis induction in AML cells by PU-H71 does not overlap with that by the p38-MAPK pathway inhibitor. Related to Figure 3. **(A)** AML cell lines were treated with PU-H71 for up to 72 h. Cell death was determined at the indicated time-points. **(B)** Non-significant correlation was found between levels of phospho-p38 (pp38) and apoptotic sensitivity to PU-H71. Each symbol represents a leukemia cell line. **(C)** Non-significant correlation was found between apoptotic sensitivity of leukemia cell lines to p38i and apoptotic sensitivity to PU-H71. Each symbol represents a leukemia cell line. **(D)** Primary AML cells with low or high sensitivity to PU-H71 were treated with the p38 inhibitor for 48 h. Percent viable cells were determined by flow cytometry (annexin V/7-AAD assay).

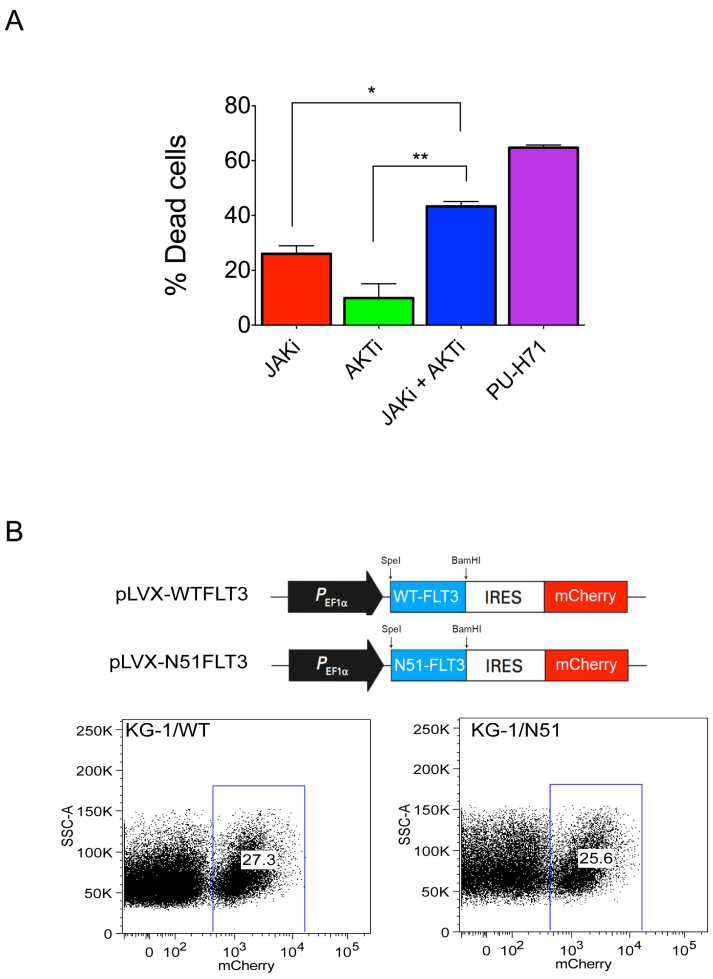

Figure S4. Simultaneous inhibition of JAK and AKT results in increased apoptotic sensitivity. Related to Figure 4. **(A**) Percent dead cells in FL5.12 cells after 48h treatment with JAKi, AKTi or PU-H71**. (B) Lentiviral constructs encoding WT-FLT3 or N51-FLT3 used to transduce KG-1 cells.** (top) schematic representation of the lentiviral vector pLVX-EF1α-IRES-mCherry harboring wild type FLT3 (WT-FLT3) or FLT3-ITD (N51-FLT3). (bottom) representative flow cytometry analysis for mCherry+ KG-1 cells.

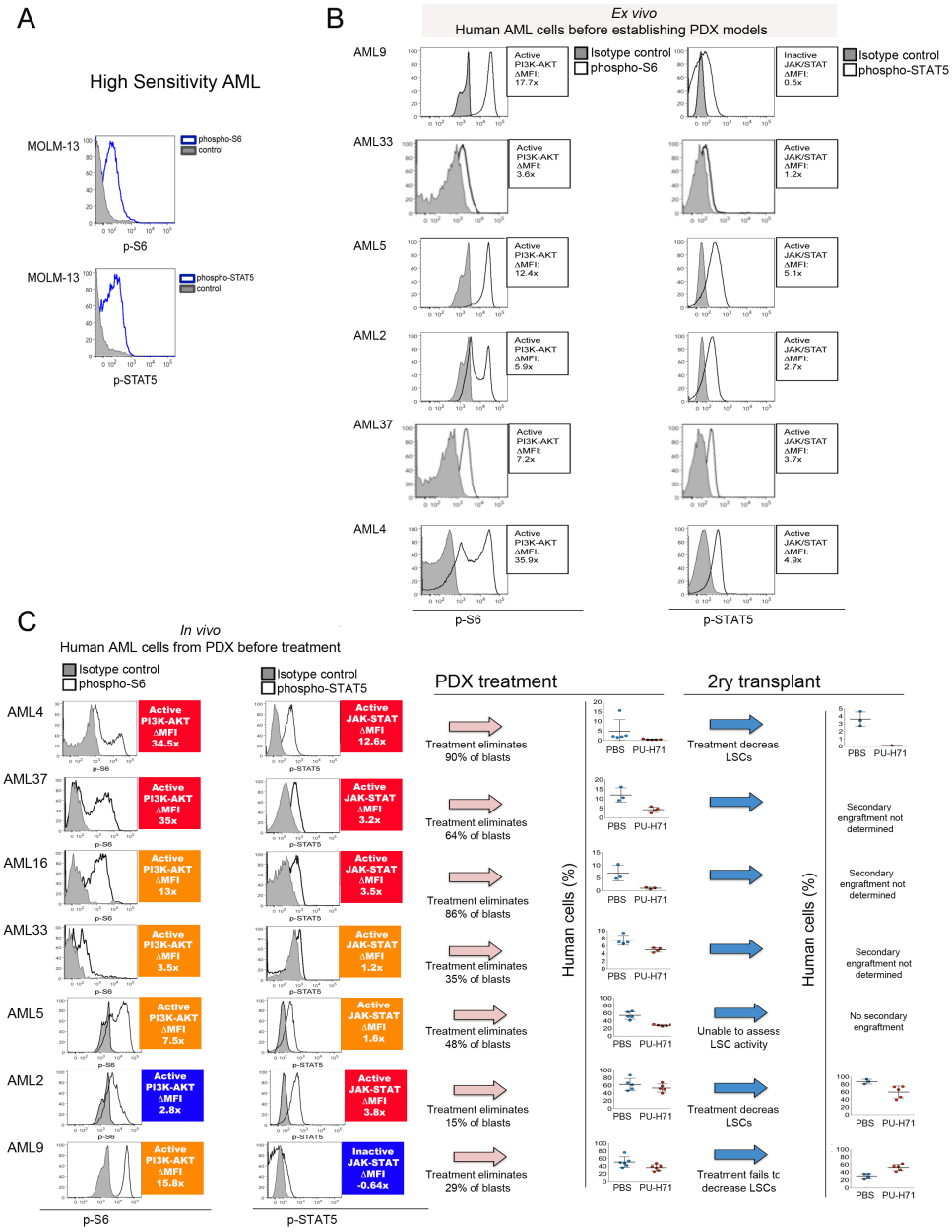

Figure S5. MOLM-13 and primary AML samples utilized for the xenotransplant models possess different basal activation levels for PI3K-AKT and JAK-STAT pathways. Related to Figure 6. Expression of p-S6 and p-STAT5 in **(A)** MOLM-13-GFP-LUC after the transplant and primary human AML samples prior **(B)** or after **(C-left panels)** generation of the PDX mice. Empty histograms represent p-S6 or p-STAT5 stained cells, filled histograms represent the isotype control. **(C-Middle panels)** Percent human cells in PDX treated with either PBS or PU-H71 (PU). **(C-Right panels)** Percent engraftment in secondary recipients to determine LSC activity from the PDX mice treated with either PBS or PU. Each symbol represents an individual mouse; Values denote mean ± SD.

SUPPLEMENTAL METHODS

Reagents. PU-H71, PU-H71 coupled to agarose beads (PU-beads) and PU-DZ13 were synthesized and used as previously described(Moulick et al., 2011). The AKT inhibitor VIII, MEK inhibitor PD98059, and the pan-JAK inhibitor I were purchased from Calbiochem. The Hsp90 inhibitors 17-AAG and BIIB021 were purchased from Selleck Chemicals. These compounds were used at concentrations as indicated by the vendor to result in inhibition of their target pathways. All compounds, except for *in vivo* studies, were used as DMSO stocks.

Cell lines and primary cell culture. Primary cryopreserved AML samples were thawed and cultured for 1 hour at 37ºC followed by treatment as described previously (Hassane et al., 2010). MV4-11, THP-1, Kasumi-1, KG-1, HL-60, U937, TUR and Kasumi-4 leukemia cell lines were purchased from the American Type Culture Collection (ATCC), SKNO-1, M0-91, HEL and OCI-AML3 cell lines were obtained from DSMZ and were cultured in Iscove's Modified Dulbecco's Medium (IMDM; Life technologies) supplemented with 10-20% fetal bovine serum (FBS) according to culture conditions indicated by ATCC and 1% penicillin/ streptomycin (Pen/Strep; Life Technologies).

For the generation of FL5.mAKT the myristylated AKT was cloned in the doxycycline inducible vector pRevTRE (Clontech) (this clone is designated mAKT). As a control, cell were transfected with vector alone (this clone is designated Vector). To activate AKT, FL5.12-derived cell lines were pre-treated with 1 g/ml doxycycline for 18h prior to treatment with inhibitors. These lines were cultured as described previously (Karnauskas et al., 2003) using RPMI-1640 media supplemented with 20mM HEPES, 55 μM beta-mercaptoethanol (β-ME), 10% FBS media containing 0 or 1 ng/mL of murine IL-3 (Fitzgerald Industries International).

Animal Studies. Experiments were carried out under an Institutional Animal Care and Use Committee-approved protocol, and institutional guidelines for the proper and humane use of animals in research were followed.

Xenografted cell lines. Four- to 6-week-old nu/nu athymic female mice were obtained from Taconic Farms. HEL and M0-91 ($1x10^7$ cells) were subcutaneously implanted in the right flank of mice using a 20-gauge needle and allowed to reach 6-8 mm in diameter before treatment. Mice bearing M0-91 and HEL tumors were administered intraperitoneally 75 mg/kg of PU-H71 hydrochloride formulated in

sterile PBS. Animals were sacrificed by CO_2 euthanasia at 12, 24, 48, 72, and 96h post administration of PU-H71. Tumors were homogenized and proteins analyzed by western blot as previously described(Caldas-Lopes et al., 2009).

Evaluation of engraftment in NOD/SCID xenotransplants. The evaluation of human engraftment was performed as previously described (Hassane et al., 2010). Briefly, Animals were sacrificed and the bone marrow (BM) cells were harvested. The BM cells were stained with PE-Cy5 conjugated mouse CD45 (mCD45), APC-H7 conjugated human CD45 (hCD45), PE conjugated human CD33 (hCD33), Alexa Fluor 700 conjugated human CD19 (hCD19), APC conjugated human CD34 (hCD34) and PE-Cy7 conjugated human CD38 (hCD38) antibodies at room temperature for 15 min. Cells were then washed, resuspended in FACS buffer containing 1 μg/ml DAPI and analyzed by for the presence of viable human leukemic cells (DAPI-/mCD45-/hCD45+) by flow cytometry.

Mouse Colony Forming Assays. C57BL/6 mice were treated with 75 mg/kg PU-H71 by i.p. twice a week for 3 weeks. Mouse bone marrow (BM) cells were collected, and 2×10^4 BM cells were plated in Methocult M3434 medium (Stemcell Technologies). Two weeks later, the images of the colonies were captured by STEMvision (Stemcell Technologies). The colony forming units (CFU) derived from PU-H71 treated mouse BM cells were compared to those from PBS treated control mice.

Cell viability assays. *Annexin V/7-AAD staining*. AML cell lines were stained with annexin V–FITC (BD Biosciences) and 7-aminoactinomycin (7-AAD, Life technologies). For primary AML samples, cells were stained with CD34, CD38, and CD45 (BD Biosciences) prior to annexin V/7-AAD staining. At least 2×10^4 events for cell lines or 2×10^5 events for primary AML samples were collected per condition on a BD LSR II flow cytometer. Data analysis was performed using FlowJo 9.3 software for Mac OS X (TreeStar). Cells that were negative for annexin V and 7-AAD were scored as viable, and the viability was represented as the percent relative to untreated controls. *Acridine orange/ethidium bromide staining*. Cells were co-stained with a mixture of acridine orange (100 mg/ml) and ethidium bromide (100 mg/ml) added in a 1:1 ratio, followed by cell visualization and counting using a fluorescent microscope (Zeiss Axiovert). Growth Inhibition. Growth inhibition studies were performed using the alamar blue assay as previously described (Caldas-Lopes et al., 2009; Rodina et al., 2007). In

summary, experimental cultures were plated at 20,000 cells/well in microtiter plates (Corning # 3603). One column of wells was left without cells to serve as the blank control. Cells were allowed to grow overnight. The following day, growth medium having either drug or DMSO at four times the desired concentration was added to another microtiter plate (Nunc 167008) in triplicate and was serially diluted at a 1:1 ratio in the plate. The diluted drug or DMSO was then added to the plated cells in a 1:1 ratio. After 72 h, the cell growth in treated versus control wells was estimated by adding alamar blue (10% v/v of 440 μM solution of resazurin (Sigma #R7017)) and measuring fluorescence intensity after six hours. The IC_{50} was calculated as the drug concentration that inhibits cell growth by 50% compared with control growth. Y-axis values below 0% represent cell death of the starting population. All experimental data were analyzed using SOFTmax Pro 4.3.1 and plotted using Prism 4.0 (Graphpad Software Inc., San Diego, CA).

Caspase 3,7 Activation Assay. Caspase 3,7 activation studies were performed as previously described(Rodina et al., 2007). Following a 24h or 48h exposure of cells to Hsp90 inhibitors, 100 μL buffer containing 10 mM HEPES, pH 7.5, 2 mM EDTA, 0.1% CHAPS, 0.1 mg/mL PMSF, Complete Protease Inhibitor mix (#1697498; Roche), and the caspase substrate Z-DEVD-R110 (#R22120; Molecular Probes) at 25 μM was added to each well. Plates were placed on an orbital shaker to promote cell lysis and reaction. The fluorescence signal of each well was measured in an Analyst GT (Molecular Devices) microplate reader (excitation 485 nm; emission at 530 nm). The percentage increase in caspase-3,7 activity was calculated by comparison of the fluorescence reading obtained from treated versus control cells. All experimental data were analyzed using SOFTmax Pro and plotted using Prism (Graphpad Software Inc., San Diego, CA).

Immunoblots. Cells were lysed in protein lysis buffer (50 mM Tris-HCl, pH 7.5, 150 mM NaCl, 1% Triton X-100, 0.1% SDS, 15 mM $MgCl_2$, 5 mM EDTA, 5 mM β-glycerophosphate, 1 mM Na_3VO_4, 1 mM NaF, and 1% protease inhibitor cocktail (Calbiochem)) on ice for 30 minutes. Twenty micrograms of protein lysates were resolved on a 10% Bis-Tris gels (Life technologies) and transferred to an Immobilon-FL polyvinylidene difluoride (FL-PVDF) or PVDF membrane (Millipore). Membranes were probed with the following primary antibodies: Anti-AKT from rabbit (1:500, 9272; Cell Signaling), anti-phospho-AKT (Ser 473) from rabbit (1:500, 9271S; Cell Signaling), anti-RAF-1 from rabbit (1:300, sc-133; Santa Cruz Biotechnology), anti-PARP (p85 fragment) from rabbit (1:250, G7341;

Promega), anti-Bcl-xL from rabbit (1:1,000, 2762; Cell Signaling), anti-JAK2 from rabbit (1:500, 3773; Cell Signaling), anti-c-KIT from mouse (1:1,000, 3308; Cell Signaling), anti-AML1 from rabbit (1:500, 4334; Cell Signaling), anti-FLT3 from rabbit (1:1,000, 3462; Cell Signaling), anti-TRKC from rabbit (1:1,000, ab43078; Abcam), and anti-β-Actin from mouse (1:3,000, ab8227–50; Abcam). anti-ERK1/2 (1:2000, 4695), anti-phospho-ERK1/2(Thr202/Tyr204; 1:2000, 4370), anti-p38 (1:2000, 9212), anti-phospho-p38(Thr180/Tyr182; 1:2000, 4511), anti-phospho-NF-κB p65(Ser536; 1:1000, 3033), were obtained from Cell Signaling. Anti-phospho-STAT5(Tyr694; 1:1000, 611964) and anti-STAT5 (1:1000, 610191) antibodies were obtained from BD Biosciences. Anti-Hsp90 (1:3000, SC-13119), anti-NF-κB p65 (1:2000, SC-372) antibodies were obtained from Santa Cruz Biotech. Hsp70 (1:2000, SPA-810) and β-actin (1:50000, A5441) antibodies were purchased from Stressgen and Sigma-Aldrich, respectively. The membranes were then incubated with either a 1:3,000 dilution of a perioxidase-conjugated corresponding secondary or IRDye 680 goat anti-rabbit or IRDye 800CW goat anti-mouse secondary antibodies (Li-COR) at room temperature for 30 min. antibody and proteins were detected via ECL-Enhanced Chemiluminescence Detection System (Amersham Biosciences) or scanned using the Odyssey infrared imaging system (Li-COR).

Phosphoflow analysis. Phosphoflow assay was performed as described with minor modifications (Schulz et al., 2012). Cells were fixed with 4% formaldehyde (EM-grade; Electron Microscopy Sciences) at room temperature for 10 min, pelleted by centrifugation, and permeabilized by resuspending in cold PBS containing 0.1% Triton X-100 and then placed on ice for 20 min. Cells were then washed with FACS buffer (0.5% FBS in PBS) twice, and stained for 1 h with antibodies against p-AKT(pS473)-Alexa Fluor 488, p-ERK1/2(pT202/pY204)-AlexaFluor-488, p-p65(pS529)-AlexaFluor-647, p-STAT5(pY694)-PE, p-p38(pT180/pY182)-Pacific Blue antibodies (BD Biosciences), NF-kBp65-AlexaFluor-647, AKT-AlexaFluor-488 and/or p-S6(S235/236)-AlexaFluor-488 antibodies

Lentiviral transduction. Wild type FLT3 (WT-FLT3) and FLT3-ITD mutant (N51-FLT3) cDNA were PCR amplified from MSCV-WTFLT3-IRES-GFP and MSCV-N51FLT3-IRES-GFP (kindly provided by Dr. Craig Jordan) respectively. pLVX-WTFLT3-mCherry and pLVX-N51FLT3-mCherry plasmids were generated by subcloning WT-FLT3 and N51-FLT3 cDNA to the SpeI/BamHI restriction sites of pLVX-EF1-IRES-mCherry vector (Clontech). Lentiviral particles were prepared,

and lentiviral infection in KG-1 cells was performed according the manufacturer's manual. Cells were sorted for mCherry+ population at 72 h following lentiviral transduction.

Immunoprecipitation. Ten million cells were lysed in Felts buffer (20 mM HEPES, 50 mM KCl, 5 mM MgCl2, 0.01% (w/v) NP-40, freshly prepared 20 mM Na2MoO4 (pH 7.2–7.3), 5 mM β-glycerophosphate, 1 mM Na3VO4, 1 mM NaF, and 1% protease inhibitor cocktail (Calbiochem)) at 4 °C for 30 min. Total protein concentration was determined using the BCA kit (Pierce) according to the manufacturer's instructions. Immunoprecipitation was performed by mixing 500 µg total cell lysates with 3 µg FLT3 antibody or normal rabbit IgG and 50 µl Protein A/G PLUS-agarose beads (Santa Cruz) at 4 °C overnight. The beads were washed five times with Felts lysis buffer and separated by SDS-PAGE followed by immunoblotting.

Chemical precipitation/PU-beads pulldowns. Cell lysates were prepared as described in immunoprecipitation section. PU-beads or control beads containing an Hsp90 inactive chemical (2-methoxyethylamine) conjugated to agarose beads were washed three times in Felts buffer. Unless otherwise indicated, the bead conjugates (80 µl) were then incubated with cell lysates at 4 °C overnight. Following incubation, bead conjugates were washed five times with the lysis buffer and proteins in the pull-down were analyzed by western blotting.

Statistical analyses. Analyses and graphs were derived using GraphPad Prism software to evaluate significance. *p<0.05, **p<0.01, ***p<0.001 and ****p<0.0001.

REFERENCES FOR SUPPLEMENTAL INFORMATION.

Caldas-Lopes, E., Cerchietti, L., Ahn, J. H., Clement, C. C., Robles, A. I., Rodina, A., Moulick, K., Taldone, T., Gozman, A., Guo, Y*., et al.* (2009). Hsp90 inhibitor PU-H71, a multimodal inhibitor of malignancy, induces complete responses in triple-negative breast cancer models. Proceedings of the National Academy of Sciences of the United States of America *106*, 8368-8373.

Hassane, D. C., Sen, S., Minhajuddin, M., Rossi, R. M., Corbett, C. A., Balys, M., Wei, L., Crooks, P. A., Guzman, M. L., and Jordan, C. T. (2010). Chemical genomic screening reveals synergism between parthenolide and inhibitors of the PI-3 kinase and mTOR pathways. Blood *116*, 5983-5990.

Karnauskas, R., Niu, Q., Talapatra, S., Plas, D. R., Greene, M. E., Crispino, J. D., and Rudin, C. M. (2003). Bcl-x(L) and Akt cooperate to promote leukemogenesis in vivo. Oncogene *22*, 688-698.

Moulick, K., Ahn, J. H., Zong, H., Rodina, A., Cerchietti, L., Gomes DaGama, E. M., Caldas-Lopes, E., Beebe, K., Perna, F., Hatzi, K.*, et al.* (2011). Affinity-based proteomics reveal cancer-specific networks coordinated by Hsp90. Nature chemical biology *7*, 818-826.

Rodina, A., Vilenchik, M., Moulick, K., Aguirre, J., Kim, J., Chiang, A., Litz, J., Clement, C. C., Kang, Y., She, Y.*, et al.* (2007). Selective compounds define Hsp90 as a major inhibitor of apoptosis in small-cell lung cancer. Nature chemical biology *3*, 498-507.

Schulz, K. R., Danna, E. A., Krutzik, P. O., and Nolan, G. P. (2012). Single-cell phospho-protein analysis by flow cytometry. Current protocols in immunology / edited by John E Coligan [et al] *Chapter 8*, Unit 8 17 11-20.